



1

2

3 Peer review status:

4 This is a non-peer-reviewed preprint submission to EarthArXiv

5 This manuscript has been submitted for publication in the journal *Ambio*.

6

7

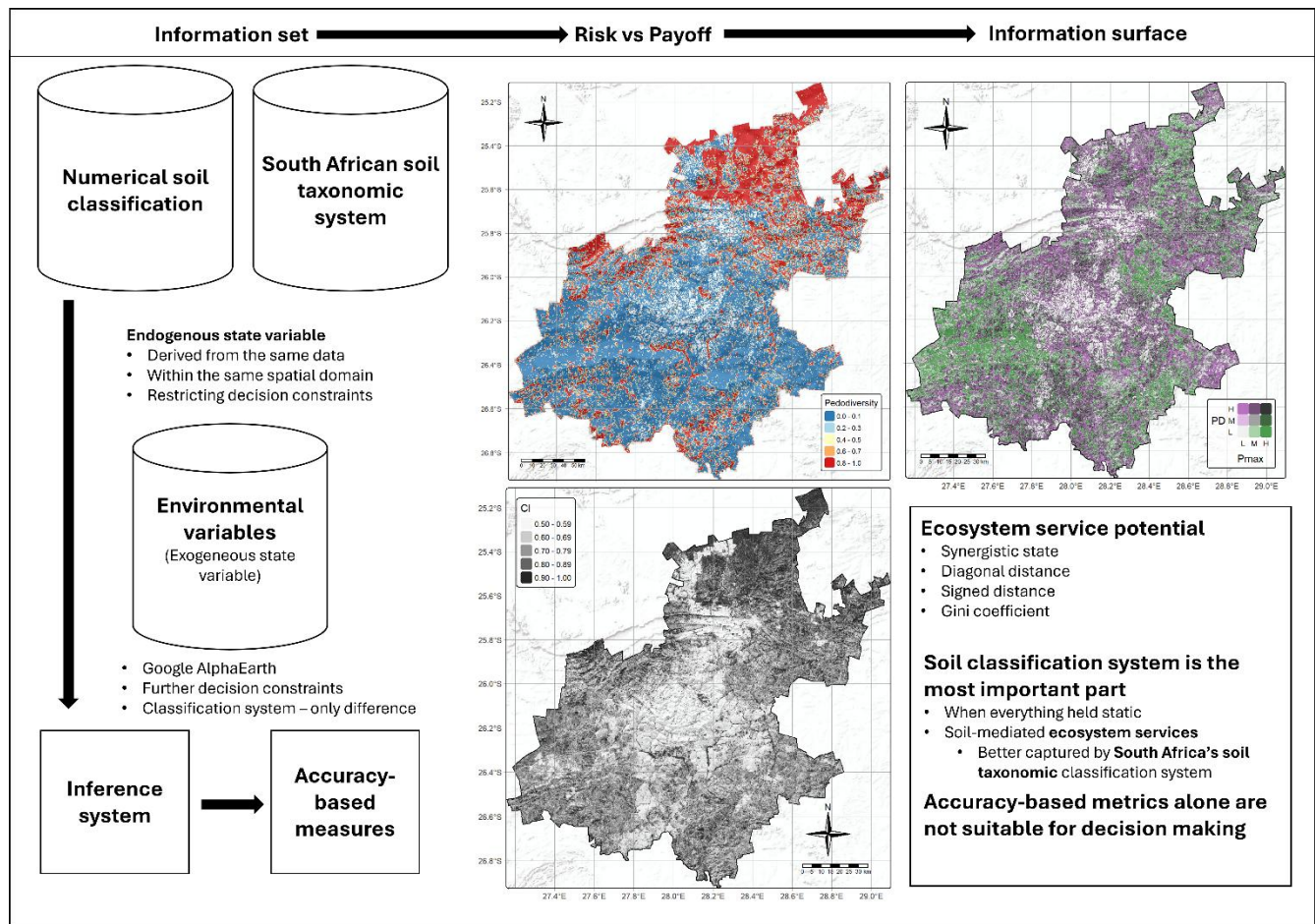
Soil-informed multivariate decision support to assess urban ecosystem service potential

Trevan Flynn^{1,2}

¹Department of Agronomy, The University of Fort Hare, Alice, South Africa

²Department of Research, add1Technologies, 11531 Slick Rock Dr., Richmond TX 77406 USA

Corresponding email: t.flynn@add1technologies.com



22
23
24

25 **Abstract**

26 Metropolitan expansion across Africa requires robust soil information to support ecosystem
27 services and urban resilience. However, digital soil mapping often prioritises predictive
28 accuracy over identifying where information is reliable for decision making. This study evaluated
29 numerical and South African Soil Taxonomy within a decision framework to assess where
30 ecosystem service inferences can be made with confidence in Gauteng, South Africa. Although
31 both approaches achieved comparable subsoil accuracy (71% vs. 80%), their information
32 spaces differed markedly. The numerical classification captured high-frequency variation but
33 generated pedodiversity through class fragmentation, producing weakly constrained spatial
34 patterns (synergistic state = 21%). In contrast, the taxonomic system preserved pedological
35 coherence through process-based transitions, maintaining pedodiversity with higher predictive
36 confidence (synergistic state = 63%). These results show that classification choice, not
37 accuracy alone, determines where reliable soil information exists. We recommend integrating
38 classification, probability, and uncertainty into a pedologically grounded decision-support
39 framework for rapidly urbanising landscapes. Current digital soil mapping approaches prioritize
40 predictive accuracy without explicitly identifying where soil information is reliable for decision
41 making. This study demonstrates that classification structures govern the translation of
42 pedodiversity into actionable knowledge, showing that higher accuracy does not necessarily
43 yield more reliable ecosystem service inference. By integrating classification, probability, and
44 uncertainty, this work introduces a framework for identifying decision-relevant soil information
45 in rapidly urbanising landscapes.

46 .
47 **Keywords:** Decision support; Pedodiversity; Pedology; Urban soil

48

49 **1. Introduction**

50 Rapid metropolitan expansion across Africa is reshaping environmental systems at
51 unprecedented rates (Awumbila, 2017). Urban growth is frequently characterised by high
52 population density, informal settlement expansion and uneven infrastructure development,
53 placing substantial pressure on soil that sustains ecosystem services essential to urban
54 resilience and human well-being (Bhatta, 2010). Urban soil regulates stormwater and flooding
55 (Anni et al., 2020), it supports food production and soil health in urban and peri-urban agriculture
56 (Wu & Congreves, 2024), mitigates urban heat (Li & Wang, 2021), and provides materials for
57 construction (Reddi et al., 2012), cultural practices, and recreation (O’Riordan et al., 2021). At
58 the same time, industrial and mining activities and pollution are widespread in many African
59 cities, frequently contaminating soil and adjacent agricultural and natural systems, with direct
60 implications for public health and ecosystem integrity (Karthika et al., 2022).

61 Decisions about land use, infrastructure placement, green-space design and environmental
62 remediation are often made under conditions of limited, uneven and uncertain and soil
63 information (Grimm et al., 2008). Soil maps are thus not only descriptive products but also
64 strategic inputs that influence how ecosystem service potential, environmental risk and
65 management trade-offs are perceived. This places increase importance on how soil information
66 is generated, represented and interpreted, particularly where there is high population density.

67 Soil-mediated ecosystem services emerge from the direct and indirect diversity of soil across
68 space and depth (Adhikari & Hartemink, 2016; Fu et al., 2022). Pedodiversity or the spatial
69 variety of soil types, properties or gradients capture this heterogeneity and reflect the capacity
70 of soil to support multiple functions and ecosystem services (Deng et al., 2025; Ibáñez et al.,
71 1995). Topsoil hosts biological activity, carbon inputs, and nutrient cycling, while subsoils
72 regulate drainage, chemical buffering, carbon stabilization, and long-term water storage (Ferré
73 et al., 2025; Fu et al., 2022; Wen et al., 2024). In urban environments, these contrasts are
74 amplified or diminished: topsoil is often disturbed or engineered, whereas subsoils may retain
75 pedogenetic structure and continue to govern critical hydrological and geochemical functions
76 (Pouyat et al., 2020).

77 Digital soil mapping (DSM) has advanced the production of spatially explicit soil property
78 maps, including bare soil, carbon stocks and contaminant distributions (Fiorentino et al., 2025;
79 Liu et al., 2022; Villa et al., 2018). Traditional evaluation emphasizes statistical metrics such as
80 overall accuracy or Cohen’s kappa coefficient (Cohen, 1960). While necessary, these metrics

81 provide limited insight into whether mapped soil information is meaningful or reliable for
82 decision-making, particularly in urban soil that are highly modified and decoupled from classical
83 soil–landscape relationships (e.g., Anthrosols and Technosols) (Pouyat et al., 2020). Accurate
84 maps may therefore be insufficient for identifying soil multifunctional areas or balancing trade-
85 offs among ecosystem services.

86 Decision-making in soil systems occurs under incomplete and asymmetric information,
87 where the true soil organization is only partially observed and unevenly understood (Regan et
88 al., 2002). Conventional and digital classification frameworks imperfectly represent underlying
89 soil processes and spatial organization, mediating access to latent soil states and shaping
90 interpretations of ecosystem service potential (Berger, 2010; Morgan & Henrion, 1990). As a
91 result, decision-theory is rarely applied to soil classification and DSM products. Where different
92 classification systems do more than label soil: they structure pedodiversity, shape interactions
93 with ecosystem services and generate distinct decision contexts even from identical
94 observations.

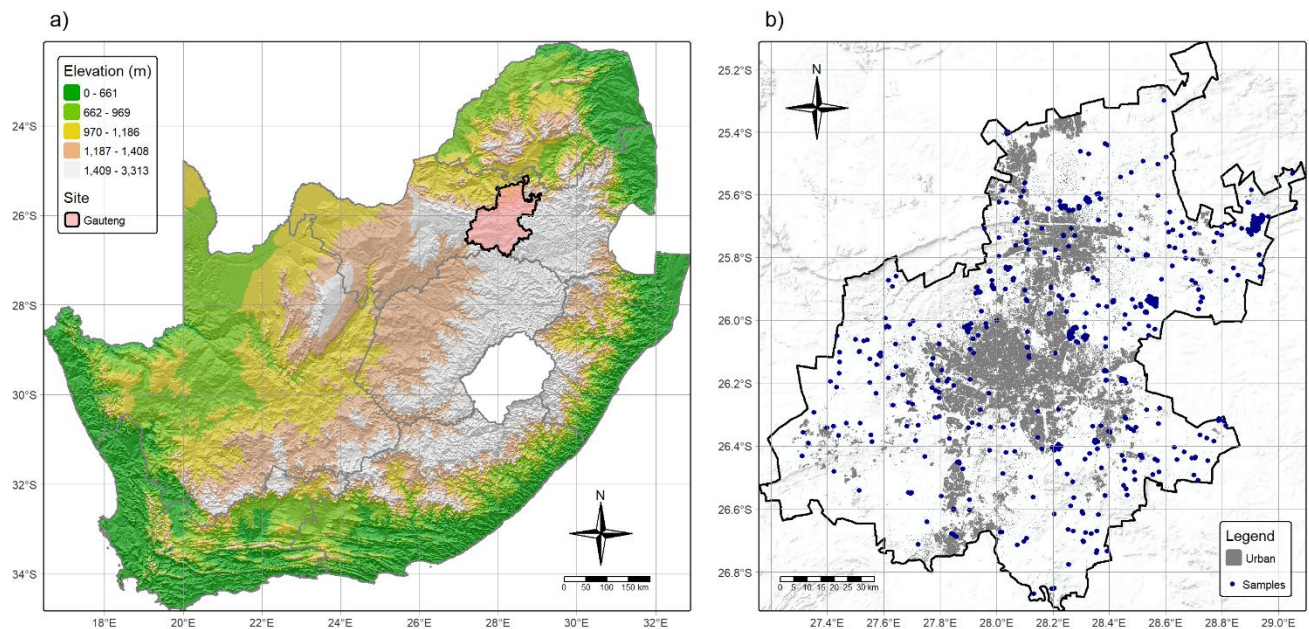
95 The aim of this study was to evaluate how a numerical and the South African taxonomic soil
96 classification systems structure ecosystem service potential in an urban landscape, specifically
97 by identifying where inferred soil information is sufficiently reliable in Gauteng Province, South
98 Africa. By treating DSM inputs and outputs as structured information that explicitly incorporates
99 uncertainty, the study emphasizes practical utility over prediction alone, highlighting how
100 classification systems influence decision-making for urban planning and ecosystem
101 management.

102 **2. Methods and materials**

103 **2.1 Study site (spatial domain, Ω)**

104 Gauteng Province (Figure 1) is located in the Highveld, a high-altitude grassland region of
105 central South Africa (approximately 26.3° S, 28.1° E). Although the smallest province by area,
106 Gauteng is the most densely populated region in the country, with an average population
107 density exceeding 850 people km⁻² (Statistics South Africa, 2016). It contains the major
108 metropolitan areas of Johannesburg and Pretoria, together with rapidly expanding cities such
109 as Soshanguve and Vereeniging. The province has a mean elevation of approximately 1,500
110 m, a mean annual temperature of ~20 °C, and a mean annual precipitation of ~650 mm (Harris
111 et al., 2020). Gauteng was selected as the study area because it represents a highly

112 heterogeneous urban–agro–natural mosaic, making it well suited for examining spatial
113 relationships between soil functions, ecosystem services, and metropolitan expansion under
114 conditions of strong anthropogenic disturbance.



115
116 *Figure 1: Gauteng Province located in South Africa (a) and Gauteng Province with major urban areas (grey) and soil*
117 *observations (b).*

118 **2.2 Data set and collection (information set, I)**

119 2.2.1 Soil data (endogenous state observations, Y)

120 Soil profile data was obtained from the South African Land Type Survey (LTS; Land Type
121 Survey Staff, 2006), comprising 565 observations (Figure 1b). The numerical classification
122 system was previously developed by Flynn et al. (2021), who clustered soil profiles into five
123 topsoil and nine subsoil classes (Table 1) using a medoid-based clustering approach.
124 Clustering was performed using the CLARA (Clustering Large Applications) algorithm, which
125 applied k-medoids clustering to identify representative medians that minimizes overall within-
126 cluster dissimilarity (Kaufman & Rousseeuw, 1986). The algorithm used Euclidean distance
127 across six chemical and five physical soil properties and was designed to provide a scalable
128 and outlier-robust classification at the national scale.

129 *Table 1: Topsoil and subsoil diagnostic horizons clustered by the Flynn et al. (2021), number of members (n) and their*
130 *properties that were observed in Gauteng.*

Horizon	Cluster	<i>n</i>	Properties
<i>Topsoil</i>	A1	36	Low clay, low SOC, mildly acidic, moderate CEC
	A2	50	High SOC, high base saturation,
	A3	404	Intermediate leaching and moderate CEC
	A4	58	High base saturation, high activity clay
	A5	17	Very high CEC and high clay
<i>Subsoil</i>	B1	181	Light texture, dominated by coarse sand
	B2	26	Light texture, dominated by fine sand
	B3	23	High clay, high CEC, mildly alkaline
	B4	15	Low CEC, moderate base saturation
	B5	237	Very high clay, slightly alkaline, high Fe
	B6	45	High clay, alkaline, high Mg
	B7	2	Coarse sand, low CEC
	B8	11	Low CEC, clay and base saturation
	B9	23	High CEC and Fe, low clay and base saturation

131

132 The LTS dataset contains modal soil profile descriptions, measured soil properties and
133 diagnostic horizons classified using the 1991 South African taxonomic “Blue Book”
134 classification (Soil Classification Working Group, 1991). The Blue Book system was used
135 because it is the most widely adopted and fully integrated classification framework within the
136 LTS at the time of analysis. For analytical consistency and interpretability, diagnostic horizon
137 names were harmonized by translating them to their closest United States Department of
138 Agriculture (USDA) Soil Taxonomy (Soil Survey Staff, 2014) equivalent or Latin descriptors,
139 and classes were grouped based on shared morphological characteristics or land-use
140 management relevance. Grouping was necessary because a large number of horizons in the
141 South African system were represented by only a single observation. Although their inclusion
142 may contribute to class imbalance and potential bias, it was necessary to preserve pedological
143 detail and maintain a comparable number of soil classes relative to the numerical classification
144 system.

145 *Table 2: Topsoil and subsoil diagnostic horizons classified by the Soil Classification Working Group, (1991), number of*
146 *members (n) and their properties that were observed in Gauteng.*

Horizon	Diagnostic	<i>n</i>	Concept
<i>Topsoil</i>	Mollic	19	High SOC, high base saturation, well structured
	Ochric	521	Topsoil that does not meet requirements of others
	Vertic	24	Swelling and cracking clay

<i>Subsoil</i>	Rhodic	199	Uniform red, slightly acidic with or without clay increase
	Xanthic	131	Uniform yellow, slightly acidic with or without clay increase
	Cambic	88	Young horizons with or without free carbonates/lithic contact
	Luvic	71	Clay increase, moderate to strong structure
	Aquic	52	Horizons that are wet for most of the year
	Plinthic	18	Horizons with clear Fe/Mn concretions (not continuous)
	Hardpan	3	Soil with a continuous hard layer
	Podzolic	3	Fe/Al and SOC accumulation with or without a Placic pan

147

148 2.2.2 Environmental variables (exogeneous state variables, X)

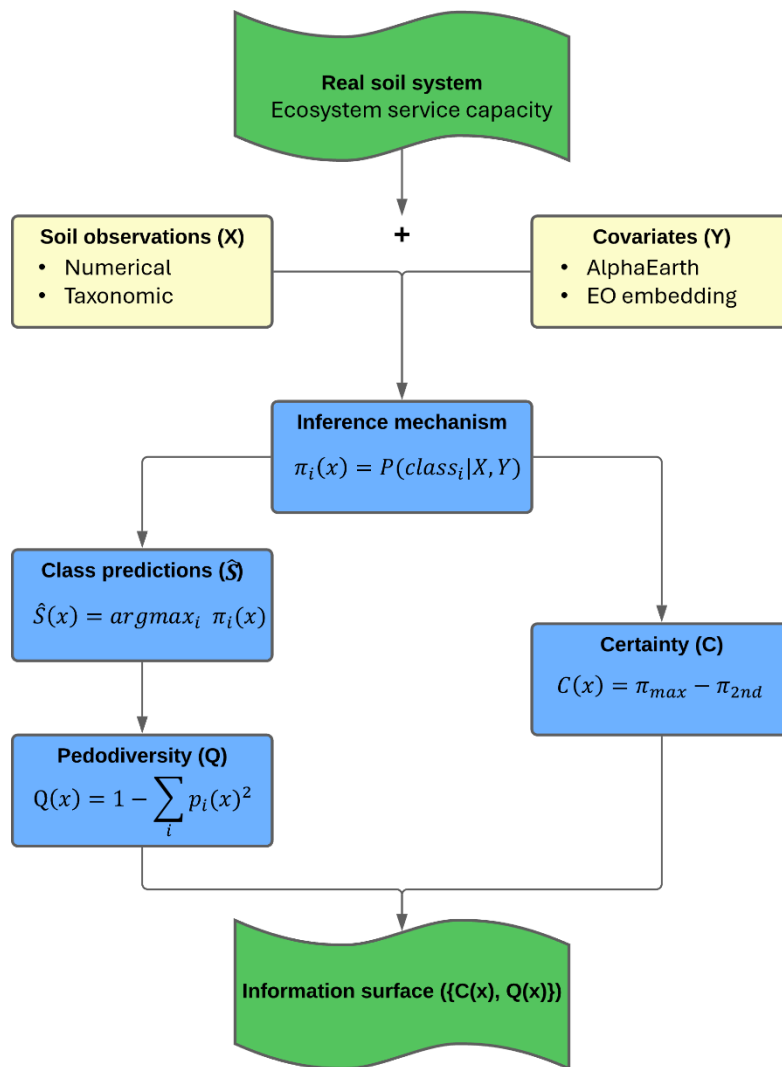
149 All 64 AlphaEarth (Brown et al., 2025) embedding layers at a 10 m spatial resolution were
 150 used for model training and spatial predictions. These embeddings are derived from multi-
 151 sensor Earth observation data and encode nonlinear representations of surface reflectance,
 152 texture and spatiotemporal context learned through self-supervised deep learning. Rather than
 153 representing individual spectral bands or indices, the embedding vectors provide a compact
 154 description of land-surface characteristics, capturing complex interactions among spectral,
 155 spatial, and temporal features. All embeddings were obtained from the median of the year 2024
 156 at a 10 m resolution and are uncorrelated so no feature selection was performed, making them
 157 suitable for spatial predictions in heterogeneous urban environments.

158 2.3 Model development

159 The mapping was implemented in a decision-making framework with incomplete information
 160 (Figure 2), in which soil classification outputs represent probabilistic surfaces about latent soil
 161 configurations and their associated ecosystem service potential. Identical soil observations (Y),
 162 environmental covariates (X), spatial domain (Ω) and the inference system (algorithm) were
 163 used for both numerical and taxonomic classification systems, ensuring that differences in
 164 outcomes reflect classification structure rather than data availability or model configuration.

165 Soil class predictions (\hat{S}) were generated through the inference mechanism (machine
 166 learning), derived from posterior class probability surfaces (π_i), which quantify the likelihood of
 167 each class at location x . Spatial predictions were therefore treated as probability distributions
 168 over soil classes rather than deterministic soil states. These probability distributions form the

169 information upon which land-use decision makers implicitly assess ecosystem service potential.
 170 Therefore, model evaluation emphasized not only predictive performance, but also the extent
 171 to which inferred patterns preserve pedological coherence and spatial structure relevant to
 172 ecosystem service interpretation.



173

174 *Figure 2: Conceptual workflow for evaluating ecosystem service potential derived from soil classification systems.*

175 2.3.1 Soil class predictions (\hat{S})

176 To predict soil classes \hat{S} , a gradient tree boosting (GTB) model was implemented in Google
 177 Earth Engine (GEE; Gorelick et al., 2017). A GTB is a generalised additive model in which base
 178 learners are small decision trees, and each successive tree corrects the residuals of the
 179 previous ensemble (Hastie et al., 2009). The construction improves regularization, accuracy
 180 and reduces overfitting (Friedman & Hastie, 1998), while nonlinear interactions enable the

181 model to capture complex relationships between soil classes and AlphaEarth covariates (Kuhn
182 & Johnson, 2013). Additionally, it is stochastic, making it well suited for modelling complex soil–
183 environment relationships (Flynn et al., 2019).

184 For each location x , posterior class probabilities $\pi_i(x)$ were produced by the model, and the
185 predicted soil class was defined as:

$$186$$
$$187 \hat{S}(x) = \operatorname{argmax}_i \pi_i(x).$$
$$188$$

189 Model performance was evaluated using an 80:20 train-test split, with predictive accuracy
190 and Cohen’s κ as accuracy-based metrics. Both classification systems were predicted with the
191 same GTB parameters of 100 sequential trees, a learning rate of 0.01 and a subsampling rate
192 of 0.7 per tree.

193 2.3.2 Uncertainties and certainties (model certainty, C)

194 Uncertainty was derived from the posterior soil-class probability distribution and calculated
195 as a confusion index (CI : Burrough et al., 1997):

$$196$$
$$197 CI = 1 - (\pi_{\max} - \pi_{2\text{nd}}),$$
$$198$$

199 where π_{\max} and $\pi_{2\text{nd}}$ denote the highest and second-highest posterior class probabilities at
200 location x . While reporting certainty is not common in soil science, it is essential here because
201 the joint behaviour of additional model outputs and potential synergistic states requires
202 quantification. Model certainty (C) was formulated as the inverse of the CI ($C = 1 - CI$). Low
203 values indicate broad probability distributions and low classification confidence, while high
204 values indicate high confidence. Certainty values were normalized to $[0, 1]$.

205

206 2.3.3 Pedodiversity (payoff, Q)

207 Pedodiversity (Q) was considered a payoff because it represents the realised capacity of a
208 landscape to support multiple soil-mediated ecosystem functions simultaneously (i.e., a
209 reward). Under the assumption that all soil types possess a dissimilarity of one, pedodiversity
210 was quantified using the Simpson Diversity Index (Simpson, 1949),

211

$$Q(x) = 1 - \sum_i p_i(x)^2,$$

212

213

214

215

216

where $p_i(x)$ represents the local proportion of soil class i within a 50 x 50 m window centred at pixel x . Proportions p_i were derived from the predicted soil classes, reflecting the spatial soil horizon patterns. The window size was thought to represent manageable land units in Gauteng’s landscape mosaic. By construction, Q captures taxonomic pedodiversity and is maximised when multiple soil classes coexist evenly within the window.

217

2.3.4 Information space ($\{C, Q\}$)

218

219

220

221

222

The joint behaviour of pedodiversity and model certainty defines a bounded information space, $\Omega = \{C(x), Q(x)\}$, within which ecosystem service outcomes were evaluated. Both quantities were normalised to the unit interval $[0, 1]$, enabling joint interpretation without scale dominance. Within this bivariate space, this relationship determines the utility of soil information for decision-making.

223

224

225

226

227

228

229

230

231

Synergistic states occur along the diagonal of this information space, where certainty and pedodiversity coincide (Table 3), indicating soil heterogeneity that is inferred with commensurate confidence. Improvements in soil classification therefore shift information toward higher joint values, expanding the region of reliable decision states. However, high pedodiversity and high certainty rarely co-occur because structural heterogeneity and inferential certainty often require opposing constraints; for example, increasing the number of soil classes often decreases classification confidence, while aggregating classes to increase certainty suppresses detectable diversity. Decision-making is thus conditioned by the synergistic region of the information space rather than by its theoretical joint maximum.

232

233

Table 3: representation of synergistic information states between model certainty (C) and pedodiversity (Q), including their statistical interpretations.

Certainty (C)	Pedodiversity (Q)	Interpretation & Decision
High	High	Stable hotspot: reliable evidence of diverse soil functions (high reward). High confidence for strategic urban planning and conservation.

Low	High	Speculative reward: high potential value but high classification risk. Information gap requires further site-specific sampling before investment.
High	Low	Predictable matrix: low diversity but high reliability. Suitable for standard, low-risk land-management protocols and infrastructure development.
Low	Low	Information void: unreliable data and low functional potential. High risk with low reward.

234

235 2.3.5 Ecosystem services potential and alignment

236 Certainty and pedodiversity were first calculated separately for each soil horizon and
 237 classification system, then summed across topsoil and subsoil to obtain profile-like measures
 238 reflecting the integrated information available from the information set (*I*). Resulting information
 239 surfaces were summarised using quantiles to support comparison across classification
 240 systems. While this aggregation does not capture full vertical profile complexity, it represents
 241 the maximum information content accessible with the given constraints.

242 Diagonal distance measures the absolute misalignment between the quantile-based C and
 243 Q classes, where values of zero indicate perfect alignment and larger values indicate increasing
 244 misalignment. Signed diagonal distance characterises the direction of this misalignment:
 245 negative values indicate Q exceeds C (high pedodiversity, low certainty), while positive values
 246 indicate C exceeds Q (low pedodiversity, high certainty). Diagonal occupancy was calculated
 247 as the proportion of pixels occupying synergistic states (low–low, mid–mid, high–high),
 248 quantifying landscape-wide concordance.

249 The Gini coefficient of diagonal distance values was used to quantify the degree of spatial
 250 alignment. Low Gini values indicate that alignment is broadly distributed across the landscape,
 251 reflecting widespread consistency between certainty and pedodiversity, whereas high Gini
 252 values indicate that alignment is spatially concentrated in specific locations, such as soil
 253 transition zones or anthropogenically disturbed urban environments (Cowell, 2011). The Gini
 254 coefficient was calculated as:

255

$$G = \frac{1}{2n^2\mu} \sum_{i=1}^n \sum_{j=1}^n |d_i - d_j|,$$

256

257

258

259

where d_i is the diagonal distance at pixel i , μ is the mean diagonal distance across all pixels, and n is the total number of pixels. Indices i and j refer to pairwise comparisons among pixels. This information space was evaluated on these parameters and spatially on the bivariate information surface that certainty and pedodiversity formed.

260

3. Results

261

3.1 Model performance

262

3.1.1 Inferred soil states

263

264

265

266

267

268

269

270

271

272

Model evaluation showed that the GTB framework produced superficially comparable predictive accuracy across both classification systems; however, accuracy-based metrics were not stable indicators of information quality (Table 4). For topsoil, numerical and taxonomic systems showed similarly high overall accuracy (87–97%) but low agreement ($\kappa = 0.24$ – 0.43), moderate confusion index (CI = 0.52 – 0.62), and a very low mean pedodiversity (Q = 0.03 – 0.09). Specifically, the numerical system exhibited lower κ and accuracy while simultaneously producing a lower confusion index, indicating that these metrics can give a misleading impression of the reliability of the spatial prediction quality. These results were not intuitive as the numerical system with the lower κ and accuracy, with the higher number of topsoil classes, had a lower uncertainty.

273

274

Table 4: Agreement (κ), accuracy, mean confusion index (CI) and mean pedodiversity (Q) of the numerical and taxonomic predictions.

System	Class	κ	Accuracy (%)	Mean CI	Mean Q
<i>Numerical</i>	Topsoil	0.24	87	0.52	0.09
	Subsoil	0.47	80	0.77	0.22
<i>Taxonomic</i>	Topsoil	0.43	97	0.62	0.03
	Subsoil	0.57	71	0.86	0.45

275

276 The subsoil results were similar to the topsoil results in that some of the metrics were
277 counter-intuitive, with the numerical system having a higher accuracy (80% vs 71%) but a lower
278 κ of 0.47 compared to 0.57. The pedodiversity was also unexpected, with a mean pedodiversity
279 of 0.22 compared to 0.45 for the taxonomic system, despite the latter having one less soil class.
280 However, several classes were not predicted under either system, with two numerical subsoil
281 classes (B7 and B8) and one taxonomic class (Vertic) absent from the model outputs.
282 Collectively, these results demonstrate that accuracy and singular metrics alone do not reflect
283 the structural and functional relevance of inferred soil patterns; rather, the soil patterns
284 themselves are influencing the discrepancies in these metrics.

285 3.1.2 Information space

286 The information surface revealed marked differences in landscape alignment between
287 classification systems (Table 5). The numerical classification exhibited a high mean diagonal
288 distance (1.15), indicating substantial misalignment between pedodiversity and certainty,
289 whereas the taxonomic system showed substantially lower misalignment (0.45). Consistent
290 with this, only 21% of the numerical system occupied synergistic states, compared with 63%
291 under the taxonomic system. Signed diagonal distance values were negative for both systems,
292 indicating a general tendency for pedodiversity to exceed confidence, but this bias was
293 markedly stronger under the numerical classification. Analysis of misalignment distribution
294 further showed that the taxonomic system localized misalignment into specific areas (Gini =
295 0.68), while the numerical system distributed misalignment more uniformly across the
296 landscape (Gini = 0.34).

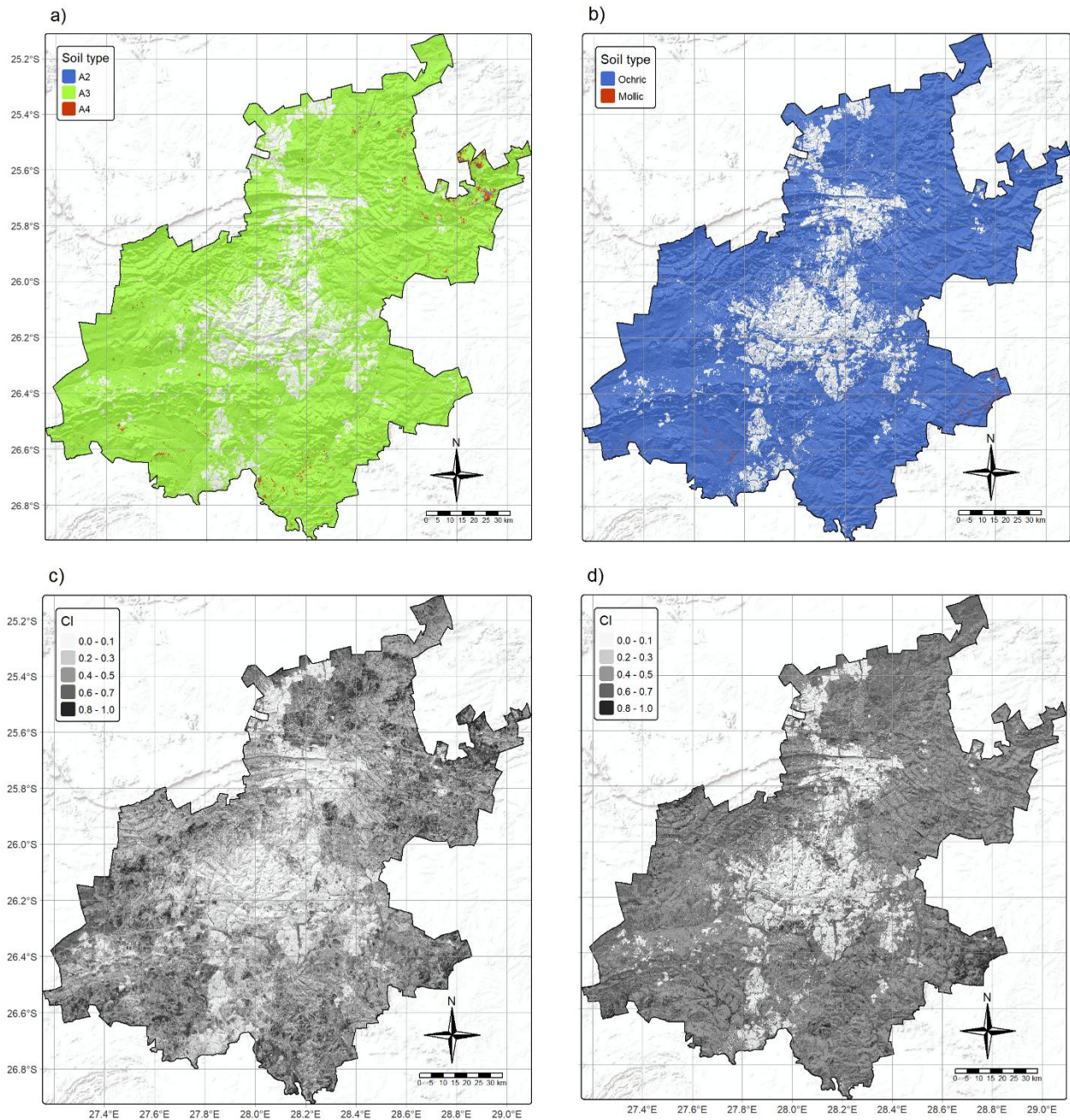
297 *Table 5: Summary of numerical and taxonomic information space showing diagonal distance, signed diagonal distance (+ or -*
298 *), area occupied by synergistic state and gini coefficient.*

Statistic	Numerical system	Taxonomic system
Diagonal distance	1.15	0.45
Signed diagonal distance	-0.78	-0.33
Synergistic state	21%	63%
Gini coefficient	0.34	0.68

300 **3.2 Spatial predictions**

301 3.2.1 Topsoil surfaces

302 Topsoil predictions, dominated by a single diagnostic horizon of A3 (96% of Gauteng) and
303 Ochric (98% of Gauteng), differed only slightly between the numerical (Figure 3a) and
304 taxonomic (Figure 3b) classification systems. In contrast, the numerical CI surface revealed
305 distinct spatial patterns with lower CI values occurring in urban and peri-urban landscapes
306 (Figure 3c). The taxonomic system, however, displayed more spatially uniform CI values with
307 higher overall magnitudes peaking in the east (Figure 3d). At this scale and resolution, small
308 patches of predictions from less predominant classes were difficult to observe.



309

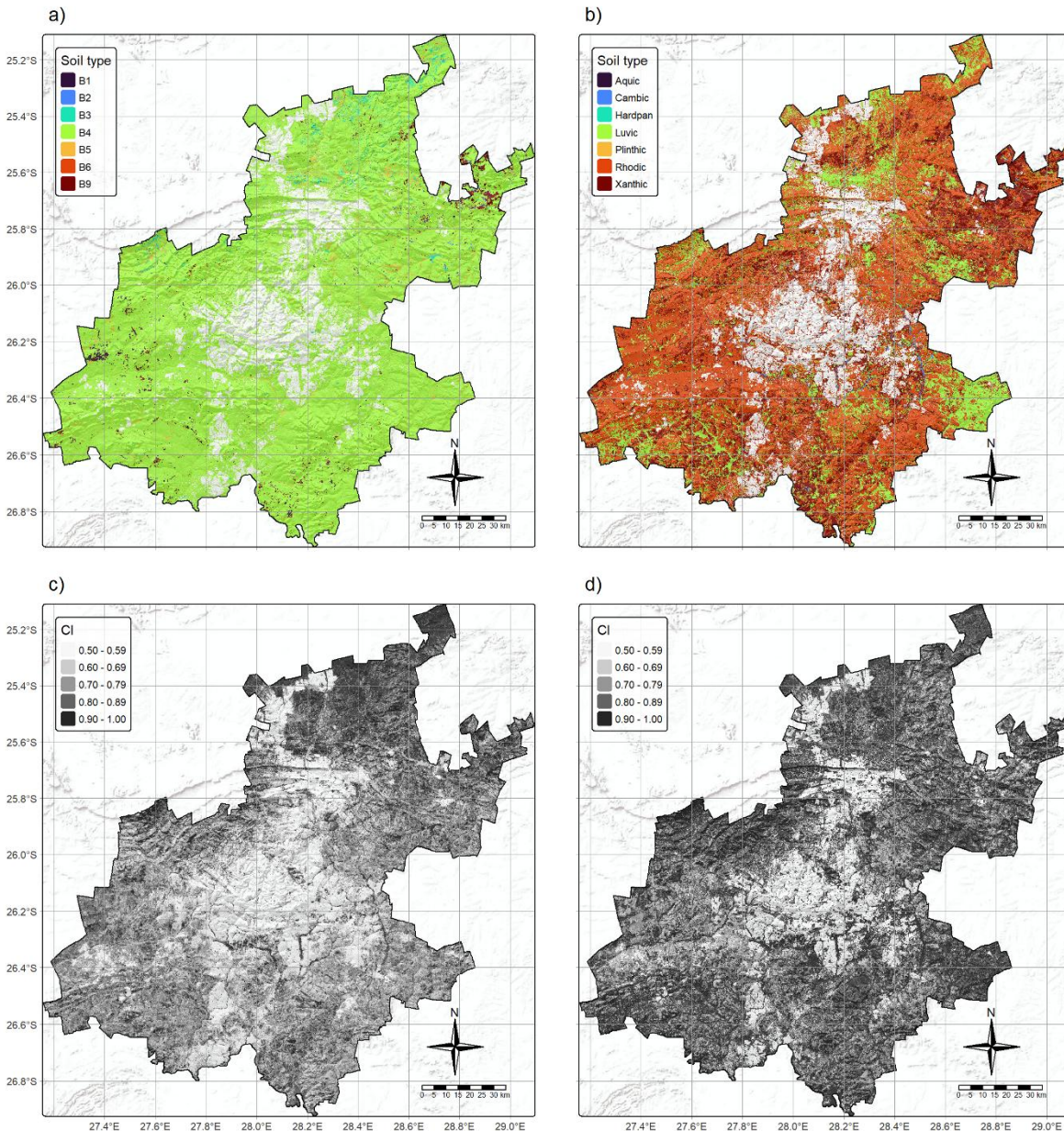
310 *Figure 3: Spatial distribution of topsoil information for Gauteng derived from the (a) numerical soil class predictions; (b)*
 311 *taxonomic soil class predictions;(c) The numerical classification uncertainty; and (d) the taxonomic classification uncertainty.*

312 **3.2.2 Subsoil surfaces**

313 Subsoil spatial predictions differed markedly between numerical and taxonomic classification
 314 systems. The numerical system produced largely homogeneous subsoil patterns dominated by
 315 a single horizon (Figure 4a) much like its topsoil counterpart. Horizon B4 occupied

316 approximately 94% of the predicted area, while the remaining classes were confined to small,
317 spatially fragmented patches. In contrast, the taxonomic system displayed multiple, spatially
318 structured subsoil horizons (Figure 4b). Rhodic horizons occupied approximately 58% of the
319 Gauteng, while Xanthic, Luvic, and Cambic horizons each accounted for substantial and
320 comparable portions ($\approx 20\%$) of the remaining landscape. The taxonomic system showed more
321 pedological relationships with Aquic horizons in valleys, Luvic in foothills, Cambic on erosion-
322 deposition positions, and Rhodic/Xanthic on more planar positions.

323 The numerical system exhibited spatially structured CI values, with higher values
324 concentrated in northern regions and lower values nearer to urban areas (Figure 4c). The
325 taxonomic system showed higher overall CI values with less spatial organisation across the
326 study area (Figure 4d). These results suggest an inverse relationship between classification
327 and uncertainty patterns: the numerical system produced spatially fragmented soil classes
328 despite having coherent uncertainty structures, whereas the taxonomic system exhibited
329 spatially coherent soil classes but disorganised uncertainty.



330

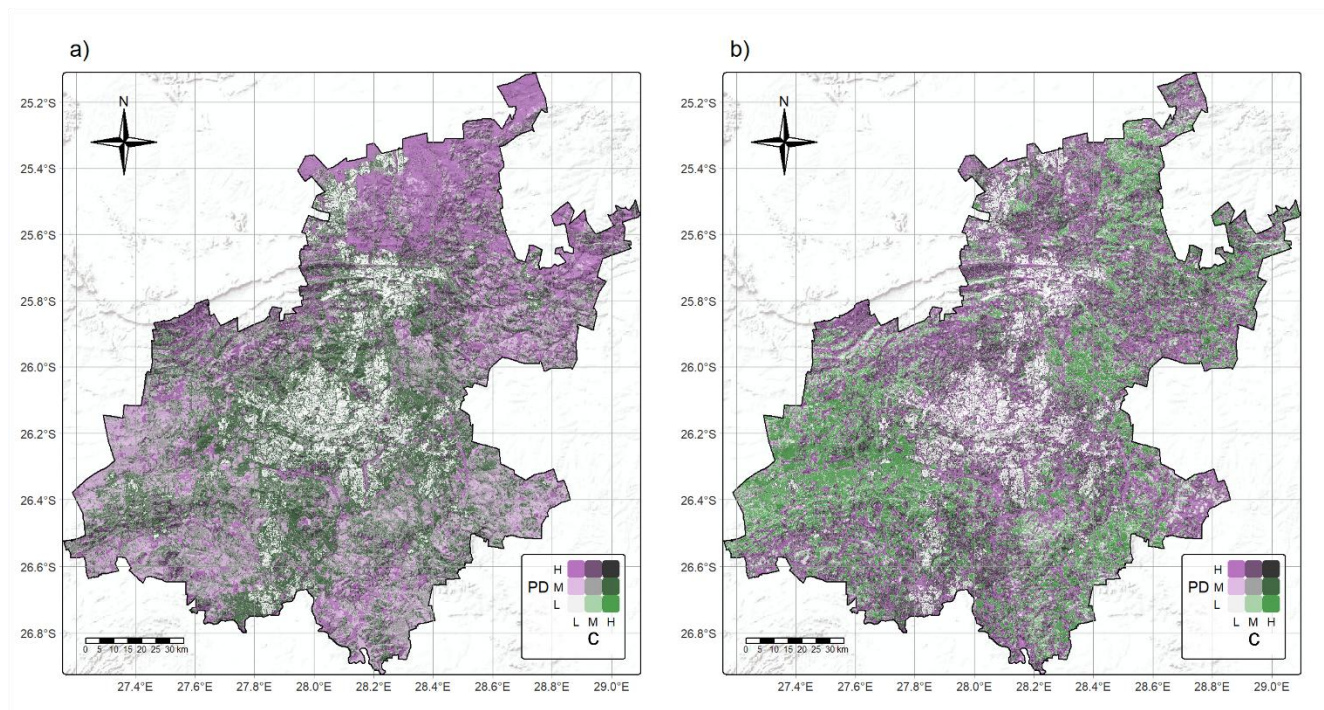
331 *Figure 4: Spatial distribution of subsoil information for Gauteng derived from the (a) numerical soil class predictions; (b)*
 332 *taxonomic soil class predictions; (c) The numerical classification uncertainty; and (d) the taxonomic classification uncertainty.*

333 3.2.3 Information surface

334 The maps of the information surfaces coincide well with the information space statistics. The
 335 combined topsoil–subsoil information surface derived from the numerical classification system
 336 revealed a strong trade-off between pedodiversity and model certainty (Figure 5a). High
 337 pedodiversity occurred predominantly where certainty was low, while areas of high certainty

338 were consistently associated with low pedodiversity. A synergistic state was rare, indicating
339 limited representation of structurally diverse soil profiles inferred with balancing confidence.

340 In contrast, the taxonomic classification system exhibited a distinctly different organisation
341 of the information space (Figure 5b). Pronounced synergistic states was evident, with extensive
342 areas where moderate to high pedodiversity coincided with moderate to high certainty. This
343 synergistic information condition forms larger and more spatially coherent patches than in the
344 numerical system. Pedodiversity patterns align with geomorphic and landscape units, and
345 certainty surfaces show corresponding spatial structure, resulting in reduced fragmentation and
346 improved spatial continuity.



347

348 *Figure 5: Information space of pedodiversity and certainty of the numerical (a) and taxonomic (b) classification systems.*

349 4. Discussion

350 Soil classes were predicted for Gauteng, South Africa, using both a numerical system and
351 the national taxonomic soil classification system. To enhance the interpretability and decision
352 relevance of these outputs, the DSM framework was reframed as a decision-making framework,
353 wherein soil maps function as information structures for ecosystem service potential under
354 uncertainty. Class predictions, posterior probabilities, and derived metrics were jointly analysed
355 to evaluate which classification system yielded greater pedodiversity (the reward) while
356 maintaining high certainty in spatial inference.

357 Overall predictive accuracy only moderately differed between classification systems, yet
358 coincided with similar studies conducted in South Africa (Flynn et al., 2025; van Zijl et al., 2019;
359 G. Van Zijl & Le Roux, 2014; G. M. Van Zijl et al., 2013). This indicates that, based on model
360 performance alone, both models would be considered reasonable outcomes. However, their
361 spatial organisation of information differed substantially. The numerical classification achieved
362 its accuracy primarily through class fragmentation, which produced significant trade-offs
363 between detail and reliability. In contrast, the taxonomic system maintained comparable
364 predictive performance while preserving spatial structure, allowing moderate to high
365 pedodiversity to be inferred with greater certainty. Collectively, these results demonstrated that
366 conventional accuracy metrics alone were insufficient for assessing the decision relevance of
367 these soil maps.

368 These differences have direct implications for urban ecosystem service assessment. In the
369 heterogeneous landscape of Gauteng, pedodiversity represents the structural capacity of soil
370 to support multifunctional services such as stormwater regulation in Pretoria (Nhamo et al.,
371 2025) or food production in peri-urban areas (Cattivelli & Pinna, 2025), while certainty reflects
372 the confidence with which this capacity can be inferred. Under the numerical system, high
373 pedodiversity is frequently associated with low certainty, particularly in areas of strong
374 anthropogenic disturbance such as soil sealing (García et al., 2014) where AlphaEarth
375 embeddings capture high spectral–spatial variability. This creates an information bottleneck,
376 limiting confidence in identifying multifunctional soil where decision support is most critical
377 affecting a large population.

378 By contrast, the taxonomic system encoded process-based transitions through diagnostic
379 horizons, enabling structurally diverse soil groups to be represented with greater spatial unity.
380 This is evidenced by the high spatial alignment of the information surface, even within the
381 complex urban fabric of Johannesburg. By filtering high-frequency surface variability that
382 disrupted numerical clustering, the taxonomic system produced a more stable information
383 structure characterized by a lower Gini coefficient. Consequently, greater confidence can be
384 placed in these synergistic states when assessing soil functions that directly affect both urban
385 and rural populations, such as erosion control (Rugendo et al., 2023), toxic pollutants (Ewis et
386 al., 2022), and crop productivity (Ma et al., 2023).

387 The limited information observed in the topsoil and numerical subsoil predictions likely
388 reflects a weak correspondence between these soil layers and the 10 m AlphaEarth

389 embeddings. In urban environments, as evidenced by the numerical system's high Gini
390 coefficient, topsoil is frequently disturbed, while subsoil classified numerically expresses
391 variability that is poorly aligned with surface-derived remote sensing. As a result, inference is
392 constrained not only by the classification but by the correlation of the information itself.
393 Expanding the information set (I), through multi-resolution covariates, depth-explicit
394 observations, or management indicators would facilitate more inferred soil states and improved
395 spatial alignment in bivariate space.

396 The prevalence of synergistic information states reflected intrinsic properties of the
397 taxonomic classification system itself. High alignment of the information surface indicates that
398 diagnostic horizons organized soil variation in a way that preserved structural heterogeneity
399 without introducing high interpretive ambiguity. In this way, synergistic states not only indicate
400 good mapping outcomes but also show how well taxonomic classes capture soil structure into
401 stable, interpretable areas. By producing frequent synergistic states, the taxonomic system
402 provided a more efficient information structure for interpreting ecosystem service potential.

403 Nevertheless, several limitations warrant investigation. Reducing complex urban soil
404 systems to bivariate dimensions may obscure finer-scale functional trade-offs, such as depth-
405 specific contaminant transport, localised soil sealing, or preferential flow in anthropogenically
406 disturbed profiles. The scale of this study may have also limited the representation of soil
407 classes within the urban–rural mosaic; a multi-resolution approach might be required to improve
408 the spatial alignment and representation of the numerical subsoil.

409 Furthermore, reliance on a static soil dataset limits the representation of rapid land-use
410 feedbacks and surface modifications characteristic of expanding metropolitan areas. While the
411 taxonomic framework successfully filtered surface noise to maintain structural consistency and
412 synergistic states, it may have missed functionally important anthropogenic soil types that the
413 "Blue Book" (Soil Classification Working Group, 1991) does not capture well. The updated
414 South African soil classification system (the "Green Book") (Soil Classification Working Group,
415 2018), however, provides more detailed diagnostics for these anthropogenic soil types, offering
416 a pathway to further improve diagonal occupancy and information utility in urbanised
417 landscapes.

418 These results demonstrate that the choice of soil classification is not a neutral modelling
419 decision, but a fundamental determinant of how raw data is transformed into actionable
420 knowledge. By framing DSM within a decision-making framework, this study showed that

421 "accuracy" is often a secondary metric to spatial alignment. In this sense, a "better map" is
422 defined not by reduced residuals, but by its ability to maximise synergistic states across the
423 landscape, providing a reliable basis for assessing ecosystem service potential in complex
424 urban–agro–natural mosaics. By favouring process-based taxonomic logic over purely
425 numerical clustering, we fundamentally expanded the decision space available to stakeholders
426 in this study. This shift from "prediction-centric" to "information-centric" mapping provided a
427 novel blueprint for navigating land-use trade-offs in an increasingly uncertain environmental
428 future within the ever-urbanising landscapes.

429 **5. Conclusion**

430 This study evaluated a numerical and South Africa's taxonomic soil classification systems
431 as information structures for assessing ecosystem service potential in the expanding
432 metropolitan landscape of Gauteng Province, South Africa. By shifting the evaluation from
433 predictive accuracy to a bivariate information space, the results showed that classification
434 choice is a primary determinant of the decision context for urban resilience. While the numerical
435 system captured multivariate variation, its high degree of class fragmentation led to weakly
436 constrained spatial patterns (synergistic state = 21%), limiting its utility for stable ecosystem
437 service inference. In contrast, the taxonomic framework preserved pedological coherence
438 through process-based transitions. This produced a fundamentally more robust information
439 structure, achieving a synergistic state of 63%. This high spatial alignment between
440 pedodiversity and certainty enables stakeholders to identify, with high confidence, the land units
441 best suited for critical functions such as erosion control, pollutant buffering and urban
442 agriculture. These findings demonstrate that "better maps" for urban governance are not
443 defined by accuracy alone, but by their capacity to provide actionable information through
444 synergistic states. Interpreting DSM outputs through this framework shifts the focus toward
445 identifying where soil information is reliable enough to support multifunctional land-use
446 decisions under uncertainty. Future research should expand this framework to diverse
447 geographic regions and modify it for specialized applications such as precision agriculture,
448 sampling regimes, or soil health monitoring; thereby operationalising the bivariate information
449 space as a versatile tool for soil resource governance.

450 .

451 **Acknowledgments**

452 We are grateful to the Agriculture Research Council-Institute of South Africa for providing
453 the data to conduct this study.

454 **References**

- 455 Adhikari, K., & Hartemink, A. E. (2016). Linking soils to ecosystem services—A global review.
456 *Geoderma*, 262, 101–111. <https://doi.org/10.1016/j.geoderma.2015.08.009>
- 457 Anni, A. H., Cohen, S., & Praskievicz, S. (2020). Sensitivity of urban flood simulations to
458 stormwater infrastructure and soil infiltration. *Journal of Hydrology*, 588, 125028–
459 125028. <https://doi.org/10.1016/j.jhydrol.2020.125028>
- 460 Awumbila, M. (2017). Drivers of Migration and Urbanization in Africa: Key Trends and Issues.
461 *UN/POP/EGM*. <https://api.semanticscholar.org>
- 462 Berger, J. O. (2010). *Statistical decision theory and Bayesian analysis* (2. ed). Springer New
463 York.
- 464 Bhatta, B. (2010). *Causes and Consequences of Urban Growth and Sprawl* (pp. 17–36).
465 https://doi.org/10.1007/978-3-642-05299-6_2
- 466 Brown, C. F., Kazmierski, M. R., Pasquarella, V. J., Rucklidge, W. J., Samsikova, M., Zhang,
467 C., Shelhamer, E., Lahera, E., Wiles, O., Ilyushchenko, S., Gorelick, N., Zhang, L. L.,
468 Alj, S., Schechter, E., Askay, S., Guinan, O., Moore, R., Boukouvalas, A., & Kohli, P.
469 (2025). *AlphaEarth Foundations: An embedding field model for accurate and efficient*
470 *global mapping from sparse label data* (arXiv:2507.22291). arXiv.
471 <https://doi.org/10.48550/arXiv.2507.22291>
- 472 Burrough, P. A., Van Gaans, P. F. M., & Hootsmans, R. (1997). Continuous classification in soil
473 survey: Spatial correlation, confusion and boundaries. *Geoderma*, 77(2–4), 115–135.
474 [https://doi.org/10.1016/S0016-7061\(97\)00018-9](https://doi.org/10.1016/S0016-7061(97)00018-9)

- 475 Cattivelli, V., & Pinna, S. (2025). Peri-urban agriculture and food platformisation: Opportunities
476 and challenges. *Journal of Rural Studies*, 115, 103568.
477 <https://doi.org/10.1016/j.jrurstud.2025.103568>
- 478 Cohen, J. (1960). A Coefficient of Agreement for Nominal Scales. *Educational and*
479 *Psychological Measurement*, 20(1), 37–46.
480 <https://doi.org/10.1177/001316446002000104>
- 481 Cowell, F. (2011). *Measuring Inequality*. Oxford University Press.
482 <https://doi.org/10.1093/acprof:osobl/9780199594030.001.0001>
- 483 Deng, G., Jiang, H., Wen, Y., He, C., Sheng, L., Gu, D., & Ma, S. (2025). Uncovering the
484 importance of soil type, landscape connectivity, and pedodiversity for nature's
485 contributions to people in a typical agricultural region. *Geoderma*, 460, 117442.
486 <https://doi.org/10.1016/j.geoderma.2025.117442>
- 487 Ewis, D., Ba-Abbad, M. M., Benamor, A., & El-Naas, M. H. (2022). Adsorption of organic water
488 pollutants by clays and clay minerals composites: A comprehensive review. *Applied Clay*
489 *Science*, 229, 106686. <https://doi.org/10.1016/j.clay.2022.106686>
- 490 Ferré, C., Mascetti, G., Gentili, R., Musetti, M., Agaba, S., & Comolli, R. (2025). The role of
491 pedodiversity in shaping biodiversity: A quantitative analysis of an alpine pasture.
492 *CATENA*, 261, 109511. <https://doi.org/10.1016/j.catena.2025.109511>
- 493 Fiorentino, A., Rajput, F. Z., Di Serio, A., Baldi, V., Guarino, F., Baldantoni, D., Ronga, D.,
494 Mazzei, P., Motta, O., Falanga, M., Cicatelli, A., & Castiglione, S. (2025). Role of Plants
495 and Urban Soils in Carbon Stock: Status, Modulators, and Sustainable Management
496 Practices. *Plants*, 14(4), 546. <https://doi.org/10.3390/plants14040546>

497 Flynn, T., Clarke, C., KostECKI, R., & Rebi, A. (2025). A comparison of country-scale subsoil
498 predictions between a numeric and a taxonomic soil classification system. *Geoderma*
499 *Regional*, 40, e00902. <https://doi.org/10.1016/j.geodrs.2024.e00902>

500 Flynn, T., de Clercq, W., Rozanov, A., & Clarke, C. (2019). High-resolution digital soil mapping
501 of multiple soil properties: An alternative to the traditional field survey? *South African*
502 *Journal of Plant and Soil*, 1–11. <https://doi.org/10.1080/02571862.2019.1570566>

503 Friedman, J., & Hastie, T. (1998). *Additive Logistic Regression: A Statistical View of Boosting*.

504 Fu, T., Liu, J., Jiang, G., Gao, H., Qi, F., & Wang, F. (2022). Influences of pedodiversity on
505 ecosystem services in a mountainous area. *CATENA*, 217, 106505.
506 <https://doi.org/10.1016/j.catena.2022.106505>

507 García, P., Pérez, M. E., & Guerra, A. (2014). Using TM images to detect soil sealing change
508 in Madrid (Spain). *Geoderma*, 214–215(May 2010), 135–140.
509 <https://doi.org/10.1016/j.geoderma.2013.09.017>

510 Gorelick, N., Hancher, M., Dixon, M., Ilyushchenko, S., Thau, D., & Moore, R. (2017). Google
511 Earth Engine: Planetary-scale geospatial analysis for everyone. *Remote Sensing of*
512 *Environment*, 202, 18–27. <https://doi.org/10.1016/j.rse.2017.06.031>

513 Grimm, N. B., Faeth, S. H., Golubiewski, N. E., Redman, C. L., Wu, J., Bai, X., & Briggs, J. M.
514 (2008). Global Change and the Ecology of Cities. *Science*, 319(5864), 756–760.
515 <https://doi.org/10.1126/science.1150195>

516 Harris, I., Osborn, T. J., Jones, P., & Lister, D. (2020). Version 4 of the CRU TS monthly high-
517 resolution gridded multivariate climate dataset. *Scientific Data*, 7(1).
518 <https://doi.org/10.1038/s41597-020-0453-3>

519 Hastie, T., Tibshirani, R., & Friedman, J. (2009). *The Elements of Statistical Learning* (2nd ed.).
520 Springer Series in Statistics.

521 Ibáñez, J. J., De-Albs, S., Bermúdez, F. F., & García-Álvarez, A. (1995). Pedodiversity:
522 Concepts and measures. *CATENA*, 24(3), 215–232. <https://doi.org/10.1016/0341->
523 8162(95)00028-Q

524 Karthika, V., Sekaran, U., Jainullabudeen, G. B., & Nagarathinam, A. (2022). Advances in
525 bioremediation of industrial wastewater containing metal pollutants. In *Biological*
526 *Approaches to Controlling Pollutants* (pp. 163–177). Elsevier.
527 <https://doi.org/10.1016/B978-0-12-824316-9.00001-X>

528 Kaufman, L., & Rousseeuw, P. J. (1986). CLUSTERING LARGE DATA SETS. In *Pattern*
529 *Recognition in Practice* (pp. 425–437). Elsevier. <https://doi.org/10.1016/B978-0-444->
530 87877-9.50039-X

531 Kuhn, M., & Johnson, K. (2013). *Applied Predictive Modeling* (p. 595). Springer New York.
532 <https://doi.org/10.1007/978-1-4614-6849-3>

533 Land Type Survey Staff. (2006). *Land Types of South Africa on 1:250 000 scale*. ARC-NRE.

534 Li, P., & Wang, Z.-H. (2021). Environmental co-benefits of urban greening for mitigating heat
535 and carbon emissions. *Journal of Environmental Management*, 293, 112963–112963.
536 <https://doi.org/10.1016/j.jenvman.2021.112963>

537 Liu, Y., Meng, Q., Zhang, L., & Wu, C. (2022). NDBSI: A normalized difference bare soil index
538 for remote sensing to improve bare soil mapping accuracy in urban and rural areas.
539 *CATENA*, 214, 106265–106265. <https://doi.org/10.1016/j.catena.2022.106265>

540 Ma, Y., Woolf, D., Fan, M., Qiao, L., Li, R., & Lehmann, J. (2023). Global crop production
541 increase by soil organic carbon. *Nature Geoscience*, 16(12), 1159–1165.
542 <https://doi.org/10.1038/s41561-023-01302-3>

543 Morgan, M. G., & Henrion, M. (1990). *Uncertainty: A Guide to Dealing with Uncertainty in*
544 *Quantitative Risk and Policy Analysis* (1st ed.). Cambridge University Press.
545 <https://doi.org/10.1017/CBO9780511840609>

546 Nhamo, G., Chapungu, L., & Mutanda, G. W. (2025). Trends and impacts of climate-induced
547 extreme weather events in South Africa (1920–2023). *Environmental Development*, *55*,
548 101183. <https://doi.org/10.1016/j.envdev.2025.101183>

549 O’Riordan, R., Davies, J., Stevens, C., Quinton, J. N., & Boyko, C. (2021). The ecosystem
550 services of urban soils: A review. *Geoderma*, *395*, 115076–115076.
551 <https://doi.org/10.1016/j.geoderma.2021.115076>

552 Pouyat, R. V., Day, S. D., Brown, S., Schwarz, K., Shaw, R. E., Szlavecz, K., Trammell, T. L.
553 E., & Yesilonis, I. D. (2020). Urban Soils. In R. V. Pouyat, D. S. Page-Dumroese, T.
554 Patel-Weynand, & L. H. Geiser (Eds.), *Forest and Rangeland Soils of the United States*
555 *Under Changing Conditions* (pp. 127–144). Springer International Publishing.
556 https://doi.org/10.1007/978-3-030-45216-2_7

557 Reddi, L. N., Jain, A. K., & Yun, H.-B. (2012). Soil materials for earth construction: Properties,
558 classification and suitability testing. In *Modern Earth Buildings* (pp. 155–171). Elsevier.
559 <https://doi.org/10.1533/9780857096166.2.155>

560 Regan, H. M., Colyvan, M., & Burgman, M. A. (2002). A taxonomy and treatment of uncertainty
561 for ecology and conservation biology. *Ecological Applications*, *12*(2), 618–628.
562 [https://doi.org/10.1890/1051-0761\(2002\)012%255B0618:ATATOU%255D2.0.CO;2](https://doi.org/10.1890/1051-0761(2002)012%255B0618:ATATOU%255D2.0.CO;2)

563 Rugendo, M. K., Gichimu, B. M., Mugwe, J. N., Mucheru-Muna, M., & Mugendi, D. N. (2023).
564 Surface runoff and soil erosion from Nitisols and Ferralsols as influenced by different soil
565 organic carbon levels under simulated rainfall conditions. *Heliyon*, *9*(7), e17684.
566 <https://doi.org/10.1016/j.heliyon.2023.e17684>

567 Simpson, E. H. (1949). Measurement of Diversity. *Nature*, 163(4148), 688–688.
568 <https://doi.org/10.1038/163688a0>

569 Soil Classification Working Group. (1991). *Soil Classification: A Taxonomic System for South*
570 *Africa* (2nd ed.). Department of Agricultural Development.

571 Soil Classification Working Group. (2018). *Soil Classification: A Natural System for South*
572 *Africa*.

573 Soil Survey Staff. (2014). *Keys to soil taxonomy* (12th ed., p. 410). USDA-Natural Resources
574 Conservation Service, Washington, DC.

575 Statistics South Africa. (2016). *Technical Report* (p. 71).

576 Van Zijl, G., & Le Roux, P. (2014). Creating a conceptual hydrological soil response map for
577 the Stevenson Hamilton Research Supersite, Kruger National Park, South Africa. *Water*
578 *SA*, 40(2), 331–336. <https://doi.org/10.4314/wsa.v40i2.15>

579 Van Zijl, G. M., Le Roux, P. A., & Turner, D. P. (2013). Disaggregation of land types using
580 terrain analysis, expert knowledge and GIS methods. *South African Journal of Plant and*
581 *Soil*, 30(2014), 123–129. <https://doi.org/10.1080/02571862.2013.806679>

582 van Zijl, G., van Tol, J., Tinnefeld, M., & Le Roux, P. (2019). A hillslope based digital soil
583 mapping approach, for hydro-pedological assessments. *Geoderma*, 354(July), 113888–
584 113888. <https://doi.org/10.1016/j.geoderma.2019.113888>

585 Villa, P., Malucelli, F., & Scalenghe, R. (2018). Multitemporal mapping of peri-urban carbon
586 stocks and soil sealing from satellite data. *Science of The Total Environment*, 612, 590–
587 604. <https://doi.org/10.1016/j.scitotenv.2017.08.250>

588 Wen, H., Wang, T., Zhang, T., & Xue, Q. (2024). Footprint of soil erosion effects on
589 pedodiversity at different hierarchical levels: A study across China's water erosion-prone

590 areas. *Journal of Environmental Management*, 372, 123152.
591 <https://doi.org/10.1016/j.jenvman.2024.123152>
592 Wu, Q., & Congreves, K. A. (2024). Soil health benefits associated with urban horticulture.
593 *Science of The Total Environment*, 912, 168852.
594 <https://doi.org/10.1016/j.scitotenv.2023.168852>

595
596